

Effect of Temperature on Asphaltene Precipitation in Crude Oils from Xinjiang Oilfield

Mingxuan Li, Yupeng Tian, Chuangye Wang, Cuiyu Jiang, Chaohe Yang, and Longli Zhang*

Cite This: *ACS Omega* 2022, 7, 36244–36253

Read Online

ACCESS |



Metrics & More

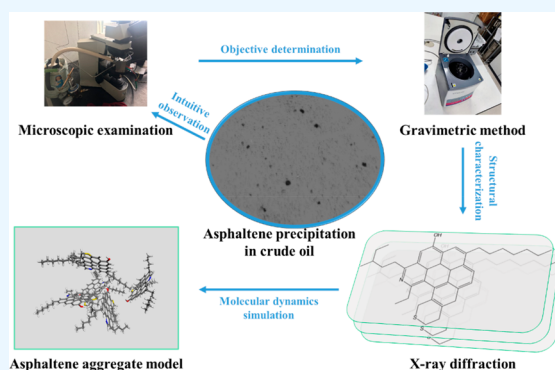


Article Recommendations



Supporting Information

ABSTRACT: During the production of crude oil, asphaltenes are prone to precipitate due to the changes of external conditions (temperature, pressure, etc.). Therefore, a series of research studies were designed to investigate the effect of temperature on asphaltene precipitation for two Xinjiang crude oils (S1, S2) so as to reveal the mechanism of asphaltene dissolution. First, the changes of asphaltene precipitation were intuitively observed by using a microscope. The results demonstrated that the asphaltene solubility increased with the increase of temperature and the dispersion rate of asphaltene particles increased with the decrease of particle size. Second, the variation of asphaltene precipitation with temperature was quantified by a gravimetric method. The results suggested that the different asphaltenes showed different sensitivity to temperature within the temperature range 25–120 °C. Third, a hypothesis was proposed to explain these results and proved that the asphaltene aggregate structure was an important factor for asphaltene stability. The crystallite parameters of asphaltenes were obtained by X-ray diffraction (XRD) to describe the structural characteristics. The results revealed that the layer distance between aromatic sheets (d_m) of asphaltenes derived from S1 oil and S2 oil were 0.378 and 0.408 nm, respectively, which implied that the asphaltene aggregates derived from S2 oil were looser than those of S1 oil. Therefore, high temperature could facilitate the penetration of resins into asphaltene aggregates and ultimately improve the dispersion of asphaltenes. Finally, molecular dynamics (MD) simulation was used to verify the conclusions. Based on the molecular dynamics method, asphaltene aggregate models were developed. The compactness and internal energy of each model were calculated. The results showed that the asphaltene dispersion capability was proportional to the porosity and internal energy.



1. INTRODUCTION

Crude oils can be divided into asphaltene, resin, aromatic, and saturate (SARA) components by solvent method.^{1,2} Asphaltenes are defined in terms of their solubility and polarity characteristics.³ Generally, the component of crude oils which is insoluble in *n*-heptane but soluble in toluene is defined as asphaltene, and no specific formula exists to express it.⁴ Asphaltenes have a complex aromatic structure, which makes them more unstable in crude oils.^{5,6} In the production of crude oils, the asphaltene stability is affected by many parameters (including pressure, temperature, etc.), and the asphaltene stability will be easily destroyed with the changes of external conditions. Once asphaltenes become unstable, they can aggregate and precipitate out of the crude oil, and in severe cases they can even clog the oil pipes in the field.⁷ The problem of asphaltene precipitation is aggravated by the great changes in temperature and pressure during the production and transportation of crude oils.

In petroleum fluid, asphaltenes are dispersed in crude oils in the form of colloid particles.⁸ The core of colloidal particles are formed by asphaltene aggregates, and asphaltene aggregates are surrounded by resins to form stable colloidal particles.⁹

Asphaltene aggregates consist of 6–10 asphaltene monomers.¹⁰ In the asphaltene aggregates, each asphaltene monomer can be regarded as an aromatic sheet, and the stable configuration of asphaltene aggregates is a layered structure.^{11,12} In highly associated asphaltene aggregates, the intermolecular force plays a crucial role in maintaining the asphaltene stability. As a result, the association behavior of asphaltenes is easily influenced by thermodynamic parameters (temperature, pressure, etc.).

Temperature is an important parameter that can affect the asphaltene stability, and the effect of temperature on asphaltene stability is complex.^{13,14} At the macroscopic level, the temperature can affect the asphaltene solubility. The asphaltene solubility increases with the increase of temper-

Received: June 10, 2022

Accepted: September 30, 2022

Published: October 7, 2022



ature, and thus, various amounts of asphaltene precipitation for the same oil will probably be produced at different temperatures. Chandio et al.¹⁵ studied the effect of temperature on the solubility of six asphaltenes and found that the asphaltene solubility increased with the increase of temperature. Alves et al.¹⁶ demonstrated that the yield of asphaltene precipitation decreased with the increase of temperature, but high temperature also exerted a negative influence on precipitation start time. It has been demonstrated that higher temperatures improve the solubility of asphaltene but, on the other hand, increase the rate of asphaltene precipitation and aggregation. The role of viscosity on the rate of aggregation is thought to be critical in the cause of more rapid asphaltene aggregation.^{17,18} As the temperature increases, the viscosity of system decreases and the diffusion rate of asphaltene particles increases. Therefore, the aggregation rate of asphaltenes is accelerated and leads to the faster acceleration of precipitation rate. Bjoroy et al.¹⁹ demonstrated that high temperatures led to lower maximum precipitation and higher initial asphaltene precipitation.

At the microscopic level, the asphaltene stability at different temperatures can also be affected by the asphaltene aggregate structure. Wang et al.²⁰ proposed that the asphaltene structure determined the mechanism of asphaltene aggregation, and the molecules with higher aromatic nucleus showed a higher aggregation tendency. Meanwhile, the alkyl side chain will inhibit the aggregation of asphaltene molecules and affect the microstructure of asphaltene aggregates.²¹ Hunter et al.²² investigated that the steric obstruction of asphaltene molecules, which would prevent the aggregation of asphaltene molecules and finally inhibit the precipitation of asphaltenes. Meanwhile, the steric hindrance has a relatively weak effect on the resins. The resins can penetrate through the microporous structure of asphaltene aggregates and adsorb on asphaltenes under the action of van der Waals forces, thereby improving the asphaltene stability.^{23,24} Asphaltenes are existed as a form of colloidal particles in crude oils, and the resins play an important role on asphaltene stability.^{25–27} However, significantly, the differences in asphaltene structure could also lead to different stabilization effects of resins on asphaltenes. The ability of resins to penetrate into asphaltene aggregates was varied with the asphaltene structure, which means that the asphaltene aggregate structure is one of the major factors in asphaltene stability. Different methods have been developed to study the asphaltene aggregate structure, such as improved Brown-Ladner (B-L) method, X-ray diffraction (XRD), transmission electron microscopy (TEM), etc.^{28–30} Recently, with the rapid development of numerical simulation techniques, molecular dynamics (MD) simulation has certain advantages in analyzing asphaltene stability at the microscopic scale.^{31,32} Lemarchand et al.³³ developed a linear asphaltene aggregate model by MD simulations. The particle size distribution and stability of asphaltene aggregates could be predicted by this model. Sedghi et al.³⁴ confirmed that the aggregative tendency of asphaltenes in toluene was less than that in *n*-heptane by MD, due to the difference of association free energy. In addition, MD simulations has been successfully extended to describe the thermodynamic properties of asphaltenes. Rogel and Carbognani³⁵ calculated the asphaltene density of different Venezuelan crude oils. The results indicated that the asphaltene density calculated by simulation MD was within the correct range. Elkahky et al.³⁶ evaluated the asphaltene density in crude oil from an Australian oil field by

MD simulations. The research showed that MD simulations was capable of providing results with qualitatively accurate. It has been found that the asphaltene density is closely related to asphaltene solubility.^{37,38} Therefore, MD simulations could be a powerful tool for assessing asphaltene stability.

With the continuous aggregation of asphaltenes, asphaltenes will further form the aggregates with larger particle size. Reservoir crack and wellbore will be gradually blocked by the aggregates, which will seriously damage the reservoir properties and reduce the production. The research shows that asphaltene molecules still retained a strong aggregation trend even in pure solvent.³⁹ According to the research of Hemmati-Sarapardeh et al.,⁴⁰ the asphaltene structure, especially the aromaticity of asphaltene, was a decisive factor for the asphaltene particle size. Microscopic examination, dynamic light scattering and ζ -potential can be used to evaluate the particle size of asphaltene aggregates in the process of asphaltene precipitation.^{41–44}

The effect of temperature on asphaltene stability has been a hot topic of research. However, for most studies, asphaltene stability has been described based on the composition of crude oil and asphaltene solubility. Furthermore, few studies have further studied the effect of asphaltene structure on asphaltene stability from a quantitative analysis. Therefore, this study aimed to quantify the influence of asphaltene structure on asphaltene stability through experiments and MD simulations. To achieve this, first, the effect of temperature on asphaltene precipitation was evaluated using microscopic examination and a gravimetric method. The microcrystalline structural parameters of asphaltenes obtained from two crude oils were investigated and compared by XRD, and the differences between asphaltene aggregates were evaluated at the molecular level. Then, based on the molecular dynamics method, the average molecular models of asphaltenes were constructed. The porosity and internal energy of each asphaltene aggregate model were calculated to quantify the contribution of asphaltene structure to asphaltene stability at different temperatures.

2. MATERIALS AND METHODS

It is well-known that the variation of thermodynamic conditions (temperature, pressure, fluid composition, etc.) may lead to the instability of asphaltene.^{45,46} Therefore, two crude oils from the Xinjiang Oilfield (S1, S2) with substantially the same properties (as shown in Table 1) were used in this paper to minimize interference from other factors in the experiment. The effect of temperature on asphaltene precipitation was investigated using conventional microscopic examination and gravimetric method. XRD and MD simulations were used to further quantify the contribution of

Table 1. Basic Properties of Crude Oil Samples Used in This Paper

characteristic	S1 oil	S2 oil
saturates (wt %)	75.32	78.56
aromatics (wt %)	19.75	16.95
resins (wt %)	3.84	3.47
asphaltenes (wt %)	1.09	1.02
density @ 25 °C(g·cm ⁻³)	0.836	0.815
viscosity @ 20 °C(pa·s)	0.00905	0.00927
viscosity @ 40 °C(pa·s)	0.00445	0.00479
API°	36.7	37.5

asphaltene structure to asphaltene precipitation at different temperatures.

2.1. Sample Preparation and Characterization. All the reagents were purchased from Sinopharm Chemical Reagent Co., Ltd. The SARA (asphaltenes, resins, aromatics, and saturates) components of crude oils were separated by a China industry standard test method (NB/SH/T 0509-2010).⁴⁷ Specifically, the following method was used to prepare samples. First, *n*-heptane was added to the crude oil samples and completely mixed by thermal reflux, and the asphaltenes were separated from the solution through filtration. Next, the solvent in the remaining solution was removed by evaporation to obtain the asphaltene. The remaining solute was dissolved by petroleum ether and divided into three components, which were named resin, aromatic, and saturate, by alumina column chromatography. Finally, the characteristics of each component and crude oils were analyzed. The average relative molecular weight of each component was determined through vapor pressure osmometry (VPO). In addition, the crude oil samples were characterized according to standard measuring methods used for the following properties: the density of oil samples⁴⁸ and the API gravity.⁴⁹ The dynamic viscosity of crude oil samples was characterized by using a rheometer (Anton Paar MCR 302).

2.2. Microscopic Examination of Asphaltene Precipitation. The microscopic morphology of asphaltene precipitation in crude oils was observed by using a Motic BA410 model polarizing microscope under 100 times magnification. The ambient temperature was controlled via a high-precision oil-bath with small temperature fluctuations. The oil bath was brought to the desired temperature and kept stable for 30 min after the temperature reached equilibrium. The round-bottom flask containing 30 mL of crude oil samples was then placed in the oil-bath. In order to minimize the evaporation losses under the high-temperature reaction, the rubber stopper was used to seal the bottle mouth during the experiment. During the experiment, samples of 5 μ L were extracted at different time intervals and observed under the microscope. The sample images at different time intervals were recorded to judge the dissolution of asphaltene precipitation at different temperatures and times. The crude oil samples were kept at a certain rate of stirring speed during the experiment, due to the stirring speed having a certain effect on asphaltene precipitation.⁵⁰

2.3. Quantification of Asphaltene Precipitation. The gravimetric method was considered to be an effective method of determining asphaltene precipitation and the onset time.^{51,52} Therefore, the gravimetric method was used to quantify the researches in this paper so as to objectively determine the effect of temperature on asphaltene precipitation. Briefly, samples of 1.5 mL were extracted from crude oil samples at different temperatures and times. In order to determine the amount of asphaltene precipitation, the samples were centrifuged at 12000 rpm for 10 min. The supernatant was then dumped after centrifugation and 1.5 mL *n*-heptane was added for ultrasonic processing to remove the residual crude oil. This process was restated three times. The washed asphaltene samples were dried to constant weight in oven and then the asphaltene precipitation was weighed.

2.4. X-ray Diffraction Measurement. The asphaltenes obtained from crude oil samples were ground into fine powder, and the X-ray diffraction study of asphaltene powder was carried out on the Rigaku Ultima IV X-ray diffractometer. The light source of the instrument used was Cu K α ($\lambda = 0.15406$

nm) radiation with operation at 45 kV and 40 mA. The scanning angle of the measured sample was $2\theta = 10\text{--}80^\circ$, and the diffraction patterns was collected at a rate of $2\theta = 5^\circ/\text{min}$. The X-ray diffraction peak was analyzed, and the Scherrer formula and Bragg relation were used to calculate the microcrystalline parameters of asphaltenes. The microcrystalline parameters included the layer distance between aromatic sheets, the diameter of the aromatic sheet and the number of aromatic sheets in a stacked cluster.

2.5. Construction and Simulation of Asphaltene Aggregate Models. ¹H NMR was used to determine the structure of asphaltenes in crude oil samples, and the elemental composition of asphaltene, including carbon, hydrogen, sulfur, and nitrogen content, was determined (Table S1, Supporting Information). The average molecular structure parameters of asphaltenes were calculated according to the improved Brown-Ladner (B-L) method (Table S2, Supporting Information).^{53,54} Theoretically, asphaltenes by nature are a mixture of diverse compounds and the molecular structure of asphaltenes should contain all the components. However, the average molecular structure parameters of asphaltenes were generated on the basis of the average information on asphaltenes in crude oils.⁵⁵ Although the average molecular structure parameters of asphaltenes could not fully represent the structure of each asphaltene molecule, they could represent the overall characteristics of asphaltenes derived from crude oil samples in this paper. The average molecular structure of asphaltenes was constructed based on the average structural parameters. The corresponding molecular models were established based on the average molecular structure of asphaltenes. The Amorphous Cell Tools module of Materials Studio was used to establish asphaltene aggregate models (the molecular number was 5), and the Forcite Tools module was used to optimize the geometry and energy of each molecular model.^{56,57} The MD simulations in the Forcite Tools module was used to testify the rationality of asphaltene aggregate models. The force field COMPASS was used in the simulation. COMPASS is a widely used all-atomic force field, which has been successfully used to describe the aggregation behavior of asphaltenes.⁵⁸ The other dynamic simulation parameters were set as follows: the ensemble was NPT, Ewald and atom-based methods were used to calculate the electrostatic and van der Waals energy, the temperature was 298.0 K, the pressure was 0.0001 GPa, the time scale was 60 ps, the dynamic simulation was 60 000 steps with the time step being 1 fs, and the results were output every 5000 steps.

3. RESULTS AND DISCUSSION

3.1. Characteristics of Crude Oil Samples. The crude oil samples came from the same field in Xinjiang, but with different extraction wells. Table 1 shows the basic properties of the crude oil samples. It could be seen that the two crude oils were characterized by similar physicochemical properties. The crude oil samples were considered to be light crude oils with API of 36.7 and 37.5, respectively. The higher saturates content and lower resins content would make a light crude oil more susceptible to asphaltene precipitation compared to a heavy crude oil.⁵⁹ The micrographs of the initial crude oil samples at 25 $^\circ$ C are shown in Figure 1. As can be seen in Figure 1, there was a large amount of asphaltene precipitation in the initial crude oil samples.

The basic properties of each component are shown in Table 2. And the C and H contents of each component in the crude

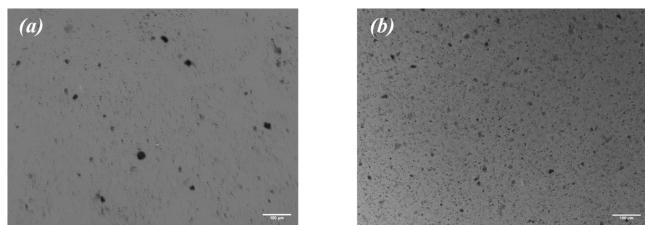


Figure 1. Micrographs of initial crude oil samples at 25 °C: (a) S1 oil and (b) S2 oil.

Table 2. Basic Properties of SARA Components of Crude Oil Samples

oil components	S1 oil		S2 oil	
	MW (g·mol ⁻¹)	N _H /N _C	MW (g·mol ⁻¹)	N _H /N _C
asphaltenes	2849	0.104	5379	0.085
resins	573	0.114	593	0.109
aromatics	346	0.118	371	0.116
saturates	303	0.167	293	0.167

oil samples were determined on the elemental analyzer (Elementar Vario EL III). As shown in Table 2, the molecular weight (MW) and N_H/N_C of resins, aromatics, and saturates derived from S1 oil were basically consistent with those of S2 oil. However, the MWs of asphaltenes derived from S2 oil were higher and the N_H/N_C values were lower. This suggested that the asphaltenes derived from S2 oil had larger a molecular weight and stronger aromaticity.

ImageJ is a program that was used to analyze the micrographs.⁶⁰ According to previous studies, the appearance of 0.5 μm particles was considered to be the onset of asphaltene precipitation.^{61,62} In this paper, the particle size was divided into three ranges of 0.5–5, 5–20, and 20–40 μm. The particle size distribution of asphaltene precipitation in the initial crude oils was analyzed, and the results are shown in Figure 2. The results showed that there was a great difference in particle size for S1 oil, and asphaltene precipitation mainly existed in S1 oil as small particles (0.5–5 μm). The particle size in S2 oil was relatively uniform, while the asphaltene precipitation was mostly distributed in 5–20 μm. Meanwhile,

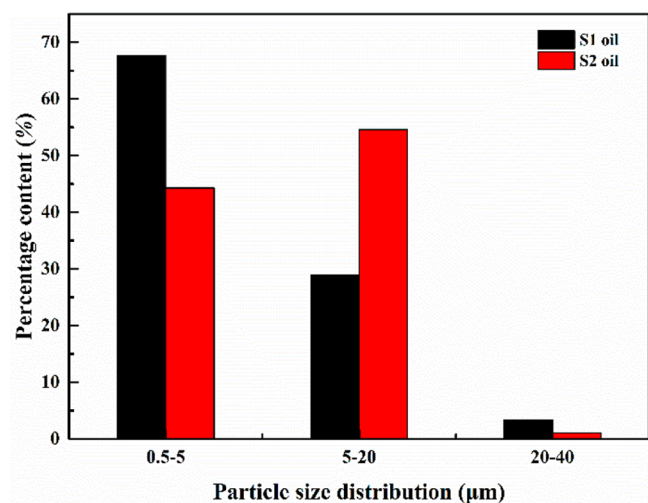


Figure 2. Particle size distribution of asphaltene particles in initial crude oil samples.

there was a small amount of large particles (20–40 μm) in both crude oil samples.

3.2. Microscopic Examination Results. Figures 3 and 4 show the micrographs of two crude oils at different

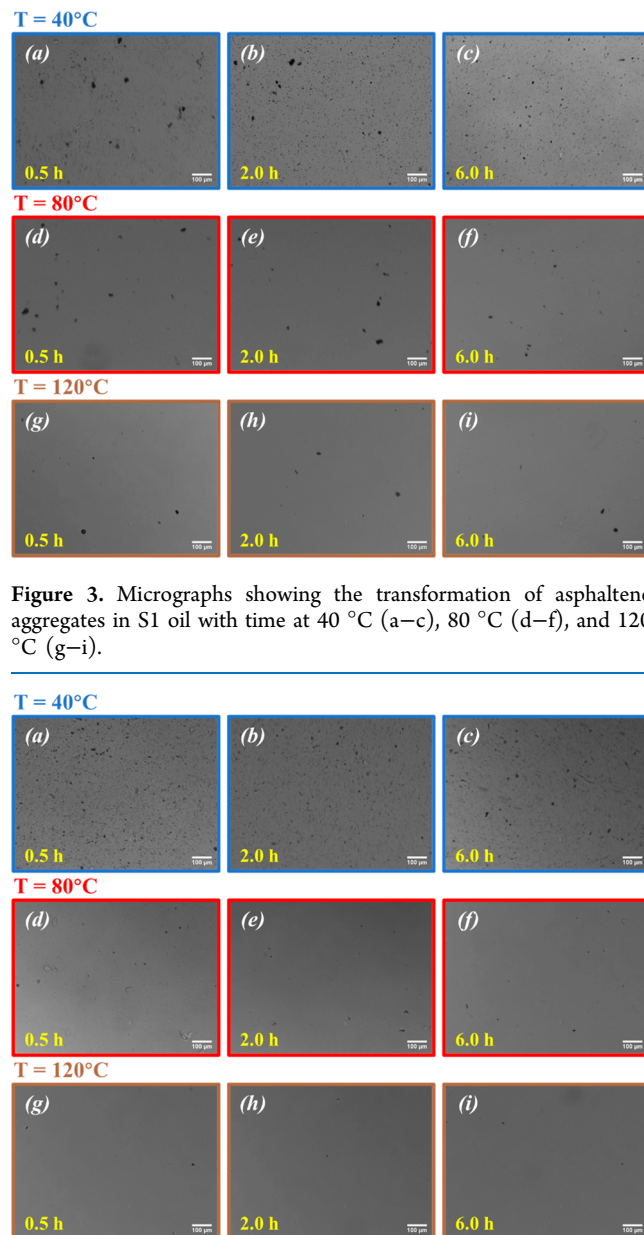


Figure 3. Micrographs showing the transformation of asphaltene aggregates in S1 oil with time at 40 °C (a–c), 80 °C (d–f), and 120 °C (g–i).

Figure 4. Micrographs showing the transformation of asphaltene aggregates in S2 oil with time at 40 °C (a–c), 80 °C (d–f), and 120 °C (g–i).

temperatures (40, 80, and 120 °C) and times (0.5, 2, and 6 h), respectively. It was clear that the dissolution of asphaltenes was improved in the process of heating. Moreover, the sensitivity of asphaltene dispersion capability to temperature was directly proportional to its particle size. This confirmed that the dispersion rate of asphaltene particles enhanced with the decrease of particle size.

The particle size distribution of asphaltene precipitation were analyzed by ImageJ. The asphaltene precipitation in the initial crude oils were regarded as reference, and the relative

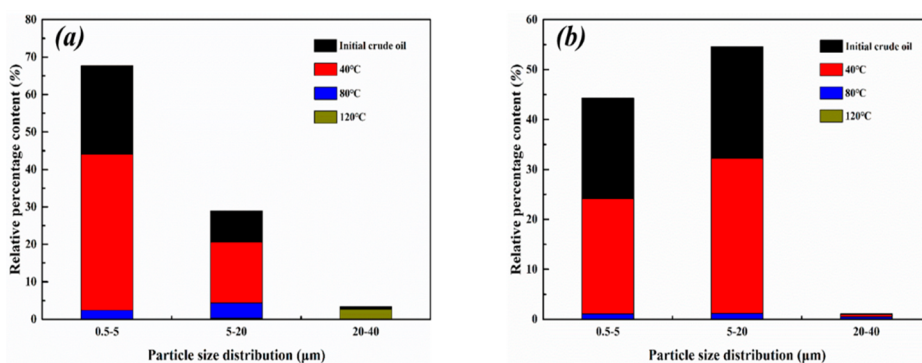


Figure 5. Particle size distribution of asphaltene particles at different temperatures: (a) S1 oil and (b) S2 oil.

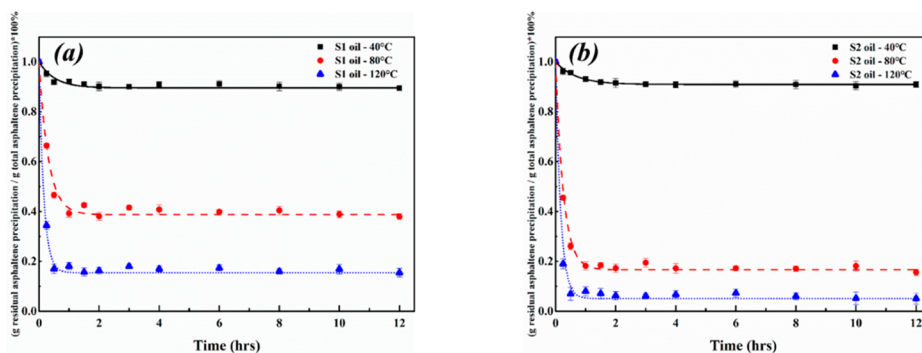


Figure 6. Mass percent of residual asphaltene precipitation with time at different temperatures: (a) S1 oil and (b) S2 oil.

changes of particle size distribution were given by the following expression:

$$w_2 = \frac{w_1}{n_1} n_2 \quad (1)$$

where w_1 is the relative content of asphaltene precipitation in the initial crude oils, w_2 is the relative content of asphaltene precipitation at certain temperature, n_1 is the number of asphaltene particles in initial crude oils, and n_2 is the number of asphaltene particles at a certain temperature. Figure 5 illustrates the relative percentage content of asphaltene particles with different particle sizes at different temperatures.

As shown in Figure 5, asphaltene particles with small sizes were more soluble, and the content of residual asphaltene precipitation decreased with the increase of temperature. In S1 oil, asphaltene particles with small particle size (0.5–5 μm) had higher dispersion efficiency. However, the asphaltene particles with large particle size (20–40 μm) were less affected by temperature and the number basically remained unchanged. In S2 oil, the asphaltene particles with particle sizes of 0.5–5 and 5–20 μm were obviously affected by temperature. Meanwhile, the asphaltene particles with a large particle size (20–40 μm) were also gradually dissolved with the increase of temperature. Microscopic observations indicated that the asphaltene solubility increased with increasing temperature, while the dispersion rate of asphaltene particles increased as the particle size decreased. In addition, the solubility of asphaltene derived from S2 crude oil was more obviously affected by temperature.

3.3. Gravimetric Examination Results. The microscopy method was subjective and prone to human errors.⁶³ Consequently, although the results of the microscopic examination appeared reasonable, it was necessary to quantify

them. The effect of temperature on asphaltene precipitation was quantified by a gravimetric method. Samples of 1.5 mL were withdrawn from the initial crude oils, and the amount of asphaltene precipitation was determined after the purification and dryness. The amount of asphaltene precipitation in the initial crude oils was regarded as the reference, and the mass percent of the remaining asphaltene precipitation in the reaction was expressed as

$$\omega = \frac{m_{\text{residual}}}{m_{\text{total}}} \times 100\% \quad (2)$$

where m_{residual} is the mass of residual asphaltene precipitation after reaction and m_{total} is the mass of asphaltene precipitation in initial crude oils.

Figure 6 shows the mass percent of the remaining asphaltene precipitation as a function of the time at different temperatures (40, 80, and 120 $^{\circ}\text{C}$). The plateau values in Figure 6 showed the percent of residual asphaltene precipitation at equilibrium. The results showed that the asphaltene solubility would be improved at higher temperatures within the experimental temperature range. Moreover, the dispersion rate of asphaltene precipitation would be enhanced with the increase of temperature.

Another conclusion drawn from Figure 6 was that the two crude oils could basically reach equilibrium after 2 h, which was consistent with the results of microscopic examination. However, after 6 h of reaction, the percent of residual asphaltene precipitation tended to slightly decrease, which might be caused by the volatilization of light components in the crude oils during repeated sampling.

By comparing the plateau values in two temperature ranges (4–80 $^{\circ}\text{C}$ and 80–120 $^{\circ}\text{C}$), it could be found that the difference of the former was greater. This result indicated that

the solubility of these asphaltenes was nonlinear with temperature in the temperature range. Therefore, the effect of temperature on asphaltene solubility was limited when the temperature exceeded a certain threshold. This finding could have important implication for field operations to control the cost effectiveness by choosing appropriate temperature range. Moreover, by comparing the plateau values in Figure 6, it was clear that temperature had a more obvious effect on the solubility of asphaltene derived from S2 oil. This result was consistent with the microscopic examination result.

Asphaltenes and resins have similar chemical properties and structural shapes, so that asphaltenes could be stabilized by resins.⁶⁴ It is well-known that the increase in the number of aromatic rings and the increase in the MW of asphaltenes would reduce the solubility of asphaltenes in crude oils.^{65,66} Although the aromaticity and MW of asphaltenes derived from S2 oil were greater than those of S1 oil, the solubility of the former was better than that of the latter. Since the properties of resins in the two crude oils were similar, the difference in asphaltene aggregate structure was speculated to be one of the major factors in asphaltene stability. Therefore, the microcrystalline parameters of asphaltenes in crude oil samples were analyzed by XRD.

3.4. X-ray Diffraction Results. The X-ray diffraction patterns of asphaltenes are shown in Figure 7. Obviously, the

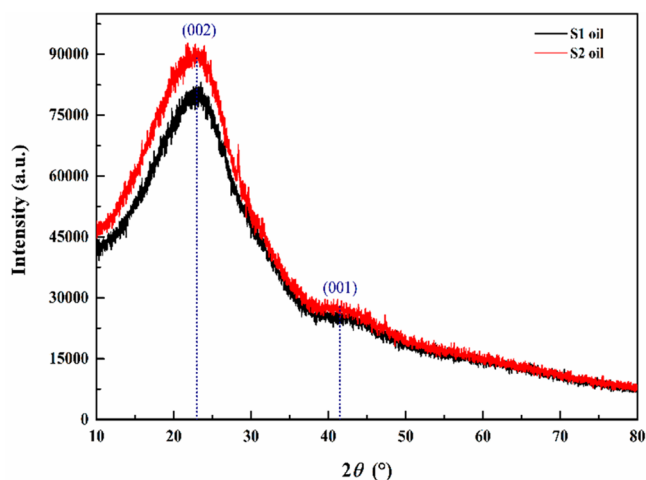


Figure 7. X-ray pattern of asphaltenes.

X-ray diffraction peaks at about $2\theta = 25^\circ$ and 42° exist in both asphaltenes due to the scattering of X-rays from the periodic molecular structure of the asphaltenes.⁶⁷ The X-ray diffraction peaks at $2\theta = 25^\circ$ and 42° are thought to represent the (002) diffraction peak and (100) diffraction peak, respectively. And the (002) diffraction peak represents the accumulation degree of aromatic sheets, while the (100) diffraction peak represents the average diameter of aromatic sheets.⁶⁸ The (002) and (100) diffraction peak shapes of the asphaltene derived from S2 oil were more significant, which indicates that there were more aromatic nuclei in the sheets, a higher aggregate degree of units, and a larger diameter of aromatic sheets. The microcrystalline parameters of asphaltenes were listed in Table 3.

As seen in Table 3, the M values of asphaltenes derived from S1 oil and S2 oil are 3.16 and 2.96, respectively, while the d_m values are 1.89 and 2.04 nm, respectively. The data indicate that the asphaltene aggregates derived from S1 oil had a greater

Table 3. Microcrystalline Parameters of Asphaltenes^a

characteristic	asphaltene of S1 oil	asphaltene of S2 oil
d_m (nm)	0.38	0.41
L_a (nm)	1.89	2.04
L_c (nm)	0.82	0.80
M	3.16	2.96

^a d_m means the layer distance between aromatic sheets. L_a means the average layer diameter of the aromatic sheets. L_c means the average height of the stack of aromatic sheets. M means the number of aromatic sheets in a stacked cluster.

number of aromatic sheets in a stacked cluster and smaller layer distance between aromatic sheets. This means that the asphaltene aggregates derived from S1 oil were more dense and condensed, while the asphaltene aggregates derived from S2 oil were relatively loose. It is well-known that the resins would penetrate into the asphaltene aggregates and adsorb on asphaltenes to improve the asphaltene stability.⁶⁹ Due to the looser structure of asphaltene aggregates derived from S2 oil, the resins could penetrate through the microporous structure of the aggregates more easily with increasing temperature. Therefore, the solubility of the asphaltene derived from S2 oil was more obviously affected by temperature. These results proved that the loose structure of asphaltene caused the asphaltene solubility more sensitive to temperature.

3.5. Construction and Simulation of Asphaltene Aggregate Models. **3.5.1. Construction of Molecular Models.** The changes of aggregate structure and other microscopic properties could be analyzed by MD simulations.^{70,71} In order to explore the mechanism of asphaltene dissolution at the molecular level, Materials Studio was used to establish the average molecular models of asphaltenes in this work. Figure 8 shows the optimal average molecular models of asphaltenes.

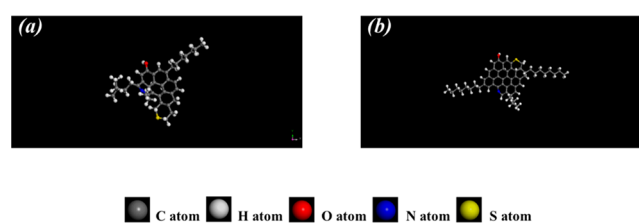


Figure 8. Optimal average molecular models of asphaltenes: (a) S1 oil and (b) S2 oil.

The size of the model (a suitable number of molecules) and a fine-enough time scale were crucial for performing MD simulations in a reasonable way.⁷² The average molecular structure of asphaltenes were constructed based on the improved Brown–Ladner (B-L) method. According to the established average molecular models of asphaltenes, assuming that the units were mainly complexed by π – π bonds, supplemented by bridge bonds and hydrogen bonds between heteroatoms. The Amorphous Cell Tools module was used to establish asphaltene aggregate models (the molecular number was 5). The results of optimizing the models are shown in Figure 9.

Due to the number of molecules in the asphaltene aggregate models (the molecular number was 5) being small, the equilibrium state of the system may not be reached after optimizing the geometry and energy of each molecular model.

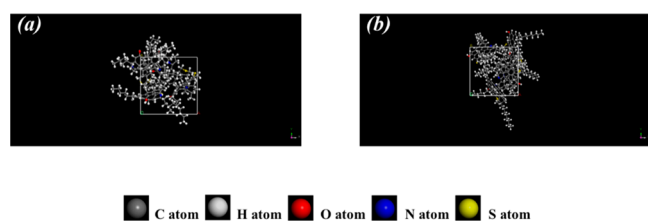


Figure 9. Optimal models of asphaltene aggregate models: (a) S1 oil and (b) S2 oil.

Therefore, in the first place, the energy and temperature of the asphaltene aggregate models were analyzed to determine whether the system was in equilibrium. The Forcite Tools module was used to calculate the energy and temperature of the models to determine whether the molecular motion in the system reached equilibrium. The simulation results are shown in Figure 10. MD simulations of the asphaltene aggregate

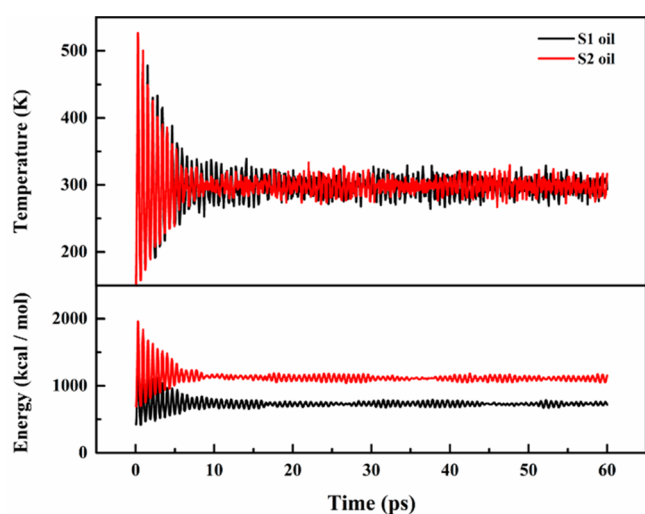


Figure 10. Relationship between energy and temperature with time of asphaltene aggregate models (1 atm, 298 K).

models showed that the fluctuation of energy and temperature in the two aggregate systems were violent in the beginning, but tended to be stable quickly on a time scale no more than 60 ps. This indicates that the molecular motion in the systems reached equilibrium. Therefore, it was appropriate to set the time scale of 60 ps for performing MD simulations.

The density is a physical property that is an important fundamental property for evaluating the rationality of the established model.^{73,74} Therefore, the density of the models was simulated to test the rationality of the models. The Forcite Tools module was used to calculate the densities of the models. The reliability of the models was verified by comparing the simulated densities with the experimental densities.

Figure 11 shows the density of the models at 1 atm and 298.0 K. It could be seen that the density fluctuated dramatically at the beginning of the simulation. However, the density of the asphaltene aggregate models changed little after 40 ps. Therefore, the density of the models were obtained by the values in 40–60 ps. The comparison results of simulated densities and experimental densities were listed in Table 4. The Experimental density in Table 4 was determined according to the method provided by Rogel et al.⁷⁵ The determinations could be accurately measured to the second decimal by this

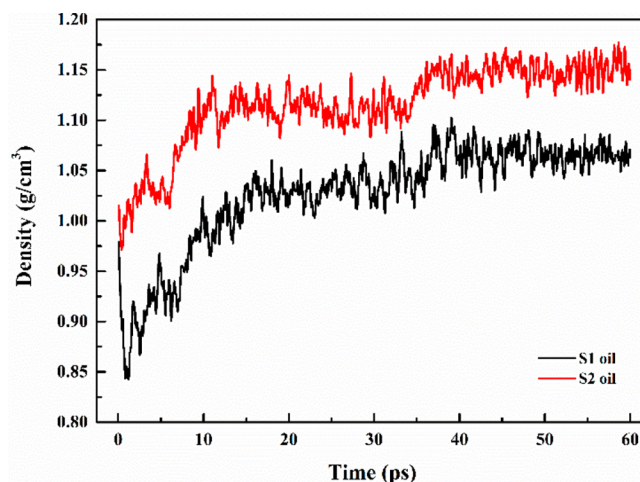


Figure 11. Density–time dependence of asphaltene aggregate models (1 atm, 298 K).

Table 4. Comparison of Simulated Densities and Experimental Densities of Asphaltene Aggregate Models (1 atm, 298 K)

asphaltenes	density (g/cm ³)		relative error (%)
	simulated density	experimental density	
S1 oil	1.066	1.08	2.11
S2 oil	1.148	1.15	−0.17

method. The simulated densities of asphaltene aggregate models were close to the experimental densities, and the relative errors were 2.11% and 0.17%, respectively. It showed that the established asphaltene aggregate models were proved to be reliable and reasonable.

3.5.2. Physical Parameters of Molecular Models. Based on the models, the PLATON software was used to calculate the porosity of asphaltene aggregate models. The porosity reflects the compactness of materials, and the unoccupied volume of materials shows a positive correlation with the porosity. The porosity (P) is the ratio of the pore volume (V_p) to the total volume (V_0) of the material in the natural state, as shown in eq 3.

$$P = \frac{V_p}{V_0} \quad (3)$$

The porosity (P) of the asphaltene aggregate models and the other relevant parameters which were obtained by Materials Studio are listed in Table 5.

Based on the data in Table 5, it could be seen that the asphaltene aggregate model in S1 oil had a smaller volume and

Table 5. Related Parameters of Asphaltene Aggregate Models (1 atm, 298 K)

characteristic	asphaltene in S1 oil	asphaltene in S2 oil
number of molecules (atoms)	5(455)	5(610)
model size (Å ³)	16.89 ³	18.95 ³
V_0 (Å ³)	4814.7	6809.8
V_f (Å ³)	829.4	1442.5
P (%)	17.22	21.18
absolute value of internal energy (kcal/mol)	18.58	97.59

fewer atoms, but the porosity (P) of the aggregate model was lower than that in S2 oil. These results indicated that the compactness of the asphaltene aggregates in S2 oil was lower in unit.

Due to the higher porosity of the asphaltene aggregate models in S2 oil, a high temperature could make the resins easier to penetrate into the aggregates. Therefore, the dispersibility and stability of the asphaltene would be further enhanced. The research showed that the internal energy was crucial for the stability of asphaltene aggregates.^{76,77} Excessive internal energy was not conducive to the stable existence of asphaltene aggregates. Therefore, the asphaltene aggregate model in S2 oil had higher internal energy. This indicated that asphaltene aggregates were thermally unstable and bind more readily to the resins as the temperature increases.

Our results showed that the structure of asphaltene aggregates was crucial for asphaltene stability. The X-ray diffraction and MD simulations provided insight into the dependence of asphaltene stability on asphaltene structure. The results showed that the loose structure of asphaltene aggregates made them more susceptible to temperature. For molecular-scale simulation, it was very important to establish an accurate molecular model of asphaltene. However, asphaltene molecular model was impossible to include all possible molecules. Therefore, the limitation of evaluating asphaltene stability by MD simulations was that the molecular models built by MD was based on the average data based on simple measurements of the whole samples.^{78,79} Even so, this work still provided the possibility of quantifying the influence of asphaltene structure on asphaltene stability, which could contribute to predicting the risk of asphaltene deposition at different temperatures.⁸⁰

4. CONCLUSIONS

In this paper, the effect of temperature on asphaltene precipitation for two Xinjiang crude oils (S1, S2) was investigated based on microscopic examination and gravimetric methods. The experiments visually showed that the asphaltene solubility increased with temperature in the temperature range 25–120 °C. Moreover, the results of the gravimetric analysis showed that the solubility of asphaltenes derived from S2 oil was more sensitive to temperature.

The structural properties of the asphaltene were correlated with asphaltene solubility by XRD and MD simulations. Based on the XRD results, the aromatic sheet of asphaltene aggregates derived from S1 oil was more dense and condensed than that of S2 oil. It meant that the high temperature could make it easier for the resins to penetrate into asphaltene aggregates derived from S2 oil and adsorb in the asphaltene aggregates. Therefore, the solubility of the asphaltenes derived from S2 oil was more obviously affected by temperature.

MD simulations were used to quantify the relationship between asphaltene stability and asphaltene aggregate structure. The molecular dynamics method was used to construct the asphaltene aggregate models, and the data revealed that the porosity (P) of the asphaltene aggregate model in S2 oil was higher. Therefore, it was easier for the resins to penetrate through the microporous structure of the asphaltene aggregates in S2 oil and further promote the disintegration of the aggregates. Moreover, the higher internal energy of the asphaltene aggregate model in S2 oil implied that the asphaltenes derived from S2 oil was less thermally stable. In this paper, the asphaltene stability not only was influenced by

the physicochemical properties (aromaticity, molecular weight, etc.) of the asphaltene, but also depended on the structural properties of the asphaltene. The study quantified the contribution of asphaltene structure to asphaltene stability at different temperatures, which is crucial for resolving asphaltene precipitation problems by selecting the appropriate temperature.

■ ASSOCIATED CONTENT

Supporting Information

The Supporting Information is available free of charge at <https://pubs.acs.org/doi/10.1021/acsomega.2c03630>.

Elemental analysis of asphaltenes in S1 oil and S2 oil; average structural parameters of asphaltenes in S1 oil and S2 oil (PDF)

■ AUTHOR INFORMATION

Corresponding Author

Longli Zhang – College of Chemistry and Chemical Engineering, China University of Petroleum (East China), Qingdao 266580, China; orcid.org/0000-0001-8546-387X; Email: llzhang@upc.edu.cn

Authors

Mingxuan Li – College of Chemistry and Chemical Engineering, China University of Petroleum (East China), Qingdao 266580, China

Yupeng Tian – College of Chemistry and Chemical Engineering, China University of Petroleum (East China), Qingdao 266580, China

Chuangye Wang – College of Chemistry and Chemical Engineering, China University of Petroleum (East China), Qingdao 266580, China

Cuiyu Jiang – College of Chemistry and Chemical Engineering, China University of Petroleum (East China), Qingdao 266580, China

Chaohe Yang – State Key Laboratory of Heavy Oil Processing, China University of Petroleum (East China), Qingdao 266580, China; orcid.org/0000-0001-6995-9170

Complete contact information is available at: <https://pubs.acs.org/10.1021/acsomega.2c03630>

Notes

The authors declare no competing financial interest.

■ ACKNOWLEDGMENTS

This work was supported by the National Natural Science Foundation of China (21576292). In addition, we also greatly appreciate the funding from the Fundamental Research Funds for the Central Universities (22CX03007A).

■ REFERENCES

- (1) Speight, J. G. The Chemistry and Technology of Petroleum. *Chem. Eng. World* **2019**, *10*, 54.
- (2) Liu, D.; Li, C.; Yang, F.; Sun, G.; You, J.; Cui, K. Synergetic effect of resins and asphaltenes on water/oil interfacial properties and emulsion stability. *Fuel* **2019**, *252* (15), 581–588.
- (3) Pereira, T. M.C.; Vanini, G.; Oliveira, E. C.S.; Cardoso, F. M.R.; Fleming, F. P.; Neto, A. C.; Lacerda, V.; Castro, E. V.R.; Vaz, B. G.; Romão, W. An evaluation of the aromaticity of asphaltenes using atmospheric pressure photoionization Fourier transform ion cyclotron resonance mass spectrometry–APPI (\pm) FT-ICR MS. *Fuel* **2014**, *118*, 348–357.

- (4) Qin, X.; Wang, P.; Sepehrnoori, K.; Pope, G. A. Modeling Asphaltene Precipitation in Reservoir Simulation. *Ind. Eng. Chem. Res.* **2000**, *39* (8), 2644–2654.
- (5) Hurt, M. R.; Borton, D. J.; Choi, H. J.; Kenttamaa, H. I. Comparison of the structures of molecules in coal and petroleum asphaltene by using mass spectrometry. *Energy Fuels* **2013**, *27* (7), 3653–3658.
- (6) Schuler, B.; Meyer, G.; Peña, D.; Mullins, O. C.; Gross, L. Unraveling the molecular structures of asphaltene by atomic force microscopy. *J. Am. Chem. Soc.* **2015**, *137* (31), 9870–9876.
- (7) Ratulowski, J.; Amin, A.; Hammami, A.; Muhammad, M.; Riding, M. Flow assurance and subsea productivity: closing the loop with connectivity and measurements. *SPE Annu. Technol. Conf. Exhib.* **2004**, SPE-90244-MS.
- (8) El-Dalatony, M. M.; Jeon, B. H.; Salama, E. S.; Eraky, M.; Kim, W. B.; Wang, J.; Ahn, T. Occurrence and characterization of paraffin wax formed in developing wells and pipelines. *Energies* **2019**, *12* (6), 967.
- (9) Goual, L.; Firoozabadi, A. Measuring asphaltene and resins, and dipole moment in petroleum fluids. *AIChE J.* **2002**, *48* (11), 2646–2663.
- (10) McKenna, A. M.; Marshall, A. G.; Rodgers, R. P. Heavy petroleum composition. 4. Asphaltene compositional space. *Energy Fuels* **2013**, *27* (3), 1257–1267.
- (11) Bouhadda, Y.; Bormann, D.; Sheu, E.; Bendedouch, D.; Krallafa, A.; Daou, M. Characterization of Algerian Hassi-Messaoud asphaltene structure using Raman spectrometry and X-ray diffraction. *Fuel* **2007**, *86* (12–13), 1855–1864.
- (12) Trejo, F.; Ancheyta, J.; Rana, M. S. Structural characterization of asphaltene obtained from hydroprocessed crude oils by SEM and TEM. *Energy Fuels* **2009**, *23* (1), 429–439.
- (13) Soroush, S.; Straver, E. J.M.; Rudolph, E. S.J.; Peters, C. J.; Loos, T. W.; Zitha, P. L.J.; Vafaie-Sefti, M. Phase behavior of the ternary system carbon dioxide + toluene + asphaltene. *Fuel* **2014**, *137* (1), 405–411.
- (14) Alves, C. A.; Yanes, J. R.; Feitosa, F. X.; Batista, H. Effect of Temperature on Asphaltene Precipitation: Direct and Indirect Analyses and Phase Equilibrium Study. *Energy Fuels* **2019**, *33* (8), 6921–6928.
- (15) Chandio, Z. A.; Ramasamy, M.; Mukhtar, H. B. Temperature effects on solubility of asphaltene in crude oils. *Chem. Eng. Res. Des.* **2015**, *94*, 573–583.
- (16) Alves, C. A.; Romero Yanes, J. F.; Feitosa, F. X.; Batista, H. Effect of Temperature on Asphaltene Precipitation: Direct and Indirect Analyses and Phase Equilibrium Study. *Energy Fuels* **2019**, *33* (8), 6921–6928.
- (17) Enayat, S.; Babu, N. R.; Kuang, J.; Rezaee, S.; Lua, H.; Tavakkoli, M.; Wang, J.; Vargas, F. M. On the development of experimental methods to determine the rates of asphaltene precipitation, aggregation, and deposition. *Fuel* **2020**, *260*, 116250.
- (18) Maqbool, T.; Srikiatiwong, P.; Fogler, H. S. Effect of Temperature on the Precipitation Kinetics of Asphaltene. *Energy Fuels* **2011**, *25* (2), 694–700.
- (19) BJORØY, Ø.; FOTLAND, P.; GILJE, E.; HØILAND, H. Asphaltene Precipitation from Athabasca Bitumen Using an Aromatic Diluent: A Comparison to Standard n-Alkane Liquid Precipitants at Different Temperatures. *Energy Fuels* **2012**, *26* (5), 2648–2654.
- (20) Wang, J.; Gayatri, M.; Ferguson, A. L. Coarse-grained molecular simulation and nonlinear manifold learning of archipelago asphaltene aggregation and folding. *J. Phys. Chem. B* **2018**, *122* (25), 6627–6647.
- (21) Murgich, J.; Abanero, J. A.; Strausz, O. P. Molecular recognition in aggregates formed by asphaltene and resin molecules from the Athabasca oil sand. *Energy Fuels* **1999**, *13* (2), 278–286.
- (22) Hunter, C. A.; Lawson, K. R.; Perkins, J.; Urch, C. J. Aromatic interactions. *J. Chem. Soc., Perkin Trans. 2* **2001**, *2* (5), 651–669.
- (23) Alvarez-Ramirez, F.; Ramirez-Jaramillo, E.; Ruiz-Morales, Y. Calculation of the interaction potential curve between asphaltene, asphaltene-resin, and resin-resin systems using density functional theory. *Energy Fuels* **2006**, *20* (1), 195–204.
- (24) Headen, T. F.; Boek, E. S.; Stellbrink, J.; Scheven, U. M. Small angle neutron scattering (SANS and V-SANS) study of asphaltene aggregates in crude oil. *Langmuir* **2009**, *25* (1), 422–428.
- (25) Anisimov, M. A.; Ganeeva, Y. M.; Gorodetskii, E. E.; Deshabo, V. A.; Kuryakov, V. N.; Yudin, D. I.; Yudin, I. K. Effects of Resins on Aggregation and Stability of Asphaltene. *Energy Fuels* **2014**, *28* (10), 6200–6209.
- (26) Sedghi, M.; Goual, L. Role of Resins on Asphaltene Stability. *Energy Fuels* **2010**, *24* (4), 2275–2280.
- (27) Yarranton, H. W.; Fox, W. A.; Svrcek, W. Y. Effect of resins on asphaltene self-association and solubility. *Can. J. Chem. Eng.* **2007**, *85* (5), 635–642.
- (28) Lipeng, H.; Bin, D.; Baoliang, P.; Jianhui, L.; Xiangfei, G.; Pingmei, W. Structure simulation and validation of Venezuela ultra heavy oil fractions. *J. Pet. Sci. Eng.* **2016**, *146*, 1173–1178.
- (29) Siddiqui, M. N.; Ali, M. F.; Shirokoff, J. Use of X-ray diffraction in assessing the aging pattern of asphalt fractions. *Fuel* **2002**, *81* (1), 51–58.
- (30) Martinez, H.; Flores, O.; Poveda, J.C.; Campillo, B. Asphaltene erosion process in air plasma: emission spectroscopy and surface analysis for air-plasma reactions. *Plasma Sci. Technol.* **2012**, *14* (4), 303.
- (31) Bai, Y.; Sui, H.; Liu, X.; He, L.; Li, X.; Thormann, E. Effects of the N, O, and S heteroatoms on the adsorption and desorption of asphaltene on silica surface: A molecular dynamics simulation. *Fuel* **2019**, *240*, 252–261.
- (32) Yao, H.; Liu, J.; Xu, M.; Ji, J.; Dai, Q.; You, Z. Discussion on molecular dynamics (MD) simulations of the asphalt materials. *Adv. Colloid Interface Sci.* **2022**, *299*, 102565.
- (33) Lemarchand, C. A.; Schröder, T. B.; Dyre, J. C.; Hansen, J. S. Coee bitumen. II. Stability of linear asphaltene nanoaggregates. *J. Chem. Phys.* **2014**, *141* (14), 144308.
- (34) Sedghi, M.; Goual, L.; Welch, W.; Kubelka, J. Effect of asphaltene structure on association and aggregation using molecular dynamics. *J. Phys. Chem. B* **2013**, *117* (18), 5765–5776.
- (35) Rogel, E.; Carbognani, L. Density estimation of asphaltene using molecular dynamics simulations. *Energy Fuels* **2003**, *17* (2), 378–386.
- (36) Elkahky, S.; Lagat, C.; Sarmadivaleh, M.; Barifcani, A. A comparative study of density estimation of asphaltene structures using group contribution methods and molecular dynamic simulations for an Australian oil field. *J. Pet. Explor. Prod. Technol.* **2019**, *9* (4), 2699–2708.
- (37) Satou, M.; Nakamura, T.; Hattori, H.; Chiba, T. Contributions of aromatic conjunction and aromatic inner carbons to molar volume of polyaromatic hydrocarbons. *Fuel* **2000**, *79* (9), 1057–1066.
- (38) Carbognani, L. Dissolution of solid deposits and asphaltene isolated from crude oil production facilities. *Energy Fuels* **2001**, *15* (5), 1013–1020.
- (39) Speight, J. G. *The chemistry and technology of petroleum*; CRC Press, 2006.
- (40) Hemmati-Sarapardeh, A.; Ameli, F.; Ahmadi, M.; Dabir, B.; Mohammadi, A. H.; Esfahanizadeh, L. Effect of asphaltene structure on its aggregation behavior in toluene-normal alkane mixtures. *J. Mol. Struct.* **2020**, *1220* (15), 128605.
- (41) Mansur, C. R.E.; Melo, A. R.; Lucas, E. F. Determination of asphaltene particle size: influence of flocculant, additive, and temperature. *Energy Fuels* **2012**, *26* (8), 4988–4994.
- (42) Haji-Akbari, N.; Teeraphakul, P.; Fogler, H. S. Effect of asphaltene concentration on the aggregation and precipitation tendency of asphaltene. *Energy Fuels* **2014**, *28* (2), 909–919.
- (43) Torkaman, M.; Bahrami, M.; Dehghani, M. Influence of temperature on aggregation and stability of asphaltene. I. Perikinetik aggregation. *Energy Fuels* **2017**, *31* (10), 11169–11180.
- (44) Hemmati-Sarapardeh, A.; Dabir, B.; Ahmadi, M.; Mohammadi, A. H.; Husein, M. M. Toward mechanistic understanding of asphaltene aggregation behavior in toluene: The roles of asphaltene

structure, aging time, temperature, and ultrasonic radiation. *J. Mol. Liq.* **2018**, *264* (15), 410–424.

(45) Zendejboudi, S.; Shafiei, A.; Bahadori, A.; James, L. A.; Elkamel, A.; Lohi, A. Asphaltene precipitation and deposition in oil reservoirs—Technical aspects, experimental and hybrid neural network predictive tools. *Chem. Eng. Res. Des.* **2014**, *92* (5), 857–875.

(46) Hammami, A.; Phelps, C. H.; Monger-McClure, T.; Little, T. M. Asphaltene precipitation from live oils: An experimental investigation of onset conditions and reversibility. *Energy Fuels* **2000**, *14* (1), 14–18.

(47) NB/SH/T 0509-2010, 2010. *Test Method for Separation of Asphalt into Four Fractions*; National Energy Administration.

(48) GB/T 13377-2010, 2010. *Crude Petroleum and Liquid or Solid Petroleum Products- Determination of Density or Relative Density-Capillary Stopped Pycnometer and Graduated Bicapillary Pycnometer Methods*; Standardization Administration.

(49) ASTM D1250-08. *Standard guide for use of the petroleum measurement tables*; ASTM International: West Conshohocken, PA, 2013.

(50) Torkaman, M.; Bahrami, M.; Dehghani, M. R. Influence of temperature on aggregation and stability of asphaltenes. II. Orthokinetic aggregation. *Energy Fuels* **2018**, *32* (5), 6144–6154.

(51) Tharanivasan, A. K.; Yarranton, H. W.; Taylor, S. D. Application of a regular solution-based model to asphaltene precipitation from live oils. *Energy Fuels* **2011**, *25* (2), 528–538.

(52) Duran, J. A.; Schoeggl, F. F.; Yarranton, H. W.; Favero, C. V.; Fogler, H. S. Effect of Air on the Kinetics of Asphaltene Precipitation from Diluted Crude Oils. *Energy Fuels* **2020**, *34* (2), 1408–1421.

(53) Zhang, J.; Tian, Y.; Qiao, Y.; Yang, C.; Shan, H. Structure and reactivity of Iranian vacuum residue and its eight group-fractions. *Energy Fuels* **2017**, *31* (8), 8072–8086.

(54) Zhang, J.; Niwamanya, N.; Gao, C.; Sekyere, D. T.; Barigye, A.; Tian, Y. Structure and millisecond pyrolysis behavior of heavy oil and its eight group-fractions on solid base catalyst. *Fuel* **2022**, *318*, 123483.

(55) Iwase, W.; Sugiyama, S.; Liang, Y.; Masuda, Y.; Morimoto, M.; Matsuoka, T.; Boek, E. S.; Ueda, R.; Nakagawa, K. Development of digital oil for heavy crude oil: molecular model and molecular dynamics simulations. *Energy Fuels* **2018**, *32* (3), 2781–2792.

(56) Su, M.; Zhou, J.; Lu, J.; Chen, W.; Zhang, H. Using molecular dynamics and experiments to investigate the morphology and microstructure of SBS modified asphalt binder. *Mater. Today Commun.* **2022**, *30*, 103082.

(57) Huang, M.; Zhang, H.; Gao, Y.; Wang, L. Study of diffusion characteristics of asphalt-aggregate interface with molecular dynamics simulation. *Int. J. Pavement Eng.* **2021**, *22* (3), 319–330.

(58) Ahmadi, M.; Chen, Z. Comprehensive molecular scale modeling of anionic surfactant-asphaltene interactions. *Fuel* **2021**, *288*, 119729.

(59) Buckley, J. S. Asphaltene deposition. *Energy Fuels* **2012**, *26* (7), 4086–4090.

(60) Collins, T. J. ImageJ for microscopy. *Biotechniques* **2007**, *43* (S1), S25–S30.

(61) Wang, J. X.; Buckley, J. S. An experimental approach to prediction of asphaltene flocculation. *SPE Int. Symp. Oilfield Chem.* **2001**, SPE-64994-MS.

(62) Maqbool, T.; Balgoa, A. T.; Fogler, H. S. Revisiting asphaltene precipitation from crude oils: A case of neglected kinetic effects. *Energy Fuels* **2009**, *23* (7), 3681–3686.

(63) Shojaei, S. A.; Osfouri, S.; Azin, R.; Dehghani, S. A. Kinetic modeling of asphaltene nano-aggregates formation using dynamic light scattering technique. *J. Pet. Sci. Eng.* **2020**, *192*, 107293.

(64) Yang, X.; Verruto, V. J.; Kilpatrick, P. K. Dynamic asphaltene-resin exchange at the oil/water interface: Time-dependent W/O emulsion stability for asphaltene/resin model oils. *Energy Fuels* **2007**, *21* (3), 1343–1349.

(65) Petrova, L. M.; Abbakumova, N. A.; Foss, T. R.; Romanov, G. V. Structural features of asphaltene and petroleum resin fractions. *Pet. Chem.* **2011**, *51* (4), 252–256.

(66) Amjad-Iranagh, S.; Rahmati, M.; Haghi, M.; Hoseinzadeh, M.; Modarress, H. Asphaltene solubility in common solvents: A molecular dynamics simulation study. *Can. J. Chem. Eng.* **2015**, *93* (12), 2222–2232.

(67) Siddiqui, M. N.; Ali, M. F.; Shirokoff, J. Use of X-ray diffraction in assessing the aging pattern of asphalt fractions. *Fuel* **2002**, *81* (1), 51–58.

(68) Jennings, J.; Growney, D. J.; Brice, H.; Mykhaylyk, O. O.; Armes, S. P. Application of scattering and diffraction techniques for the morphological characterization of asphaltenes. *Fuel* **2022**, *327*, 125042.

(69) León, O.; Contreras, E.; Rogel, E.; Dambakli, G.; Acevedo, S.; Carbognani, L.; Espidel, J. Adsorption of native resins on asphaltene particles: a correlation between adsorption and activity. *Langmuir* **2002**, *18* (13), 5106–5112.

(70) Yao, H.; Dai, Q.; You, Z. Molecular dynamics simulation of physicochemical properties of the asphalt model. *Fuel* **2016**, *164* (15), 83–93.

(71) Dong, Z.; Liu, Z.; Wang, P.; Gong, X. Nanostructure characterization of asphalt-aggregate interface through molecular dynamics simulation and atomic force microscopy. *Fuel* **2017**, *189* (1), 155–163.

(72) Chmiela, S.; Saucedo, H. E.; Poltavsky, I.; Müller, K. R.; Tkatchenko, A. sGDML: Constructing accurate and data efficient molecular force fields using machine learning. *Comput. Phys. Commun.* **2019**, *240*, 38–45.

(73) Li, B.; Liu, G.; Xing, X.; Chen, L.; Lu, X.; Teng, H.; Wang, J. Molecular dynamics simulation of CO₂ dissolution in heavy oil resin-asphaltene. *J. CO₂ Util.* **2019**, *33* (C), 303–310.

(74) Satou, M.; Nakamura, T.; Hattori, H.; Chiba, T. Contributions of aromatic conjunction and aromatic inner carbons to molar volume of polyaromatic hydrocarbons. *Fuel* **2000**, *79* (9), 1057–1066.

(75) Rogel, E.; Carbognani, L. Density estimation of asphaltenes using molecular dynamics simulations. *Energy Fuels* **2003**, *17* (2), 378–386.

(76) Martín-Martínez, F. J.; Fini, E. H.; Buehler, M. J. Molecular asphaltene models based on Clar sextet theory. *RSC Adv.* **2015**, *5* (1), 753–759.

(77) Redelius, P. G. Solubility parameters and bitumen. *Fuel* **2000**, *79* (1), 27–35.

(78) Sugiyama, S.; Liang, Y.; Murata, S.; Matsuoka, T.; Morimoto, M.; Ohata, T.; Nakano, M.; Boek, E. S. Construction, Validation, and Application of Digital Oil: Investigation of Asphaltene Association Toward Asphaltene-Precipitation Prediction. *SPE J.* **2018**, *23* (03), 952–968.

(79) Jian, C.; Liu, Q.; Zeng, H.; Tang, T. A Molecular Dynamics Study of the Effect of Asphaltenes on Toluene/Water Interfacial Tension: Surfactant or Solute? *Energy Fuels* **2018**, *32* (3), 3225–3231.

(80) Zhang, F.; Shen, B.; Sun, H.; Liu, J.; Liu, L. Rational Formulation Design and Commercial Application of a New Hybrid Solvent for Selectively Removing H₂S and Organosulfurs from Sour Natural Gas. *Energy Fuels* **2016**, *30*, 12–19.